*Materials Science-Poland, Vol. 23, No. 2, 2005*

# Multifractal description of fracture morphology: Quasi-3D analysis of fracture surface

SEBASTIAN STACH[1*], JAN CWAJNA[2], STANISŁAW ROSKOSZ[2], JERZY CYBO[1]

[1]Department of Materials Science, Silesian University, ul. Snieżna 2, 41-200 Sosnowiec, Poland

[2]Department of Materials Science, Silesian University of Technology, ul. Krasińskiego 8, 40-019 Katowice, Poland

The paper presents a verification of the multifractal analysis proposed in other papers. It has been found that the analysis of simulated profiles formed by removing overlaps and secondary cracks from a real profile (which corresponds to a file obtained from a profilographometer) ensures proper diversity of fractal characterization, adequate for the degree of fracture surface development of the investigated grades of sintered carbide measured with a Taylor–Hobson's Talysurf 2 profilographometer.

Key words: *fracture; surface; stereometry; overlaps; profile; multifractal; spectrum width*

## 1. Introduction

A quantitative characterization of a fracture constitutes an indispensable link in the investigation of the processes of decohesion and crack resistance of a material [1]. A distinguishing feature of the latter is the degree of fracture development, the evaluation of which is conducted on the basis of an analysis of a profile containing possible overlaps and secondary cracks [2]. In order to reduce laborious research procedure of preparing transverse microsections, their image analysis, and to eliminate the minimal representation resulting from examining only one to three profiles, a concept is put forward in the paper to use a profilographometer [3]. The device facilitates obtaining stereometric files of the surface topography very quickly, which permits analysis of an optional number of profiles in selected directions. Since the principle of operation of a profilographometer does not allow disclosure of the existing overlaps and cracks, a transposition by means of a multifractal analysis has been proposed [4–7]. This allowed making the multifractal spectrum spacing dependent on the degree of profile

*Corresponding author, e-mail: sstach@us.edu.pl

line development as well as on local changes of the distances between those spectrum points where overlaps and secondary cracks occur [8]. In order to check whether there is a relationship between the multifractal spectrum width and the percentage share of overlaps in real profiles, a regression analysis was made. A high correlation coefficient was obtained ($R = 0.88$) showing that the multifractal analysis of simulated profiles (without overlaps and cracks, i.e. profiles corresponding to the data from the profilographometer [9]) is fully correlated with the degree of the real profile development. Verification of the correlation coefficient allowed significance of $\alpha \leq 0.05$ for the coefficient, which shows potentiality of $\geq 95\%$ trust in relation to the possible estimation error $\delta_{0.05}$ to be assumed.

A consequence of the former stage is the transition to a morphology analysis of a real fracture in 3D [10]. The multifractal analysis methodology presented in papers [3, 8] should constitute a link between both examination methods of a profile and a whole fracture.

The purpose of this study is to show the possibility of describing the fracture development with a high level of accuracy by analyzing all mutually perpendicular profiles (quasi-3D) which form the surface of a fracture examined by stereometric methods using a profilographometer.

## 2. Tools and materials

The materials studied were seven grades of WC-Co sintered carbides having a two-phase structure: α (WC grains) + β (binding phase – Co). The criterion for the selection of grades for the research was differences of tungsten carbide grain size, from 0.5 to 8.0 μm, and various volume fractions of the cobalt phase, from 6% to 15%, as shown in Table 1.

Table 1. Chemical composition and properties of sintered carbide grades selected for the investigation

| Grade | Chemical composition | | Average diameter of WC grain, μm | Density, g/cm$^3$ | Hardness, $HV_{30}$ |
|---|---|---|---|---|---|
| | % WC | % Co | | | |
| HF6 | 94.0 | 6.0 | 0.5–0.8 | 14.9 | 1800 |
| H10 | 94.0 | 6.0 | 1.0–2.0 | 14.8 | 1600 |
| H30 | 91.0 | 9.0 | 1.0–2.0 | 14.6 | 1380 |
| G10 | 94.0 | 6.0 | 2.0–3.0 | 14.9 | 1430 |
| G30 | 85.0 | 15.0 | 2.0–3.0 | 14.0 | 1150 |
| B2 | 91.0 | 9.0 | 2.0–3.0 | 14.6 | 1250 |
| B23G | 90.5 | 9.5 | 6.0–8.0 | 14.6 | 1050 |

The fracture surfaces for the research were the outcome of a three-point static bending test, for which a specially made ZDM-2500 testing machine was used. The

tests were conducted with accurate strain measurement in the force range 0–25 kN. Samples of dimensions: $l$ = 50 mm, $b$ = 6 mm, $h$ = 10 mm were used (Figs. 1, 2).

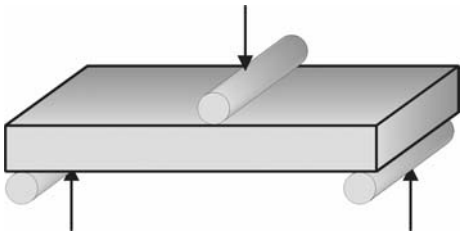

Fig. 1. Diagrammatic drawing of three-point bending of sintered carbides

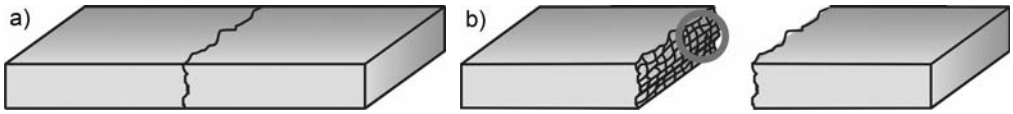


Fig. 2. Sample after three-point bending (a) and fracture surface with a marked place of stereometric analysis (b)

## 3. Results and analysis

The fracture surfaces of all sintered carbide grades were subjected to measurement using a Taylor–Hobson's Form TalySurf Series 2 profilographometer. This device (Fig. 3) is fully automated and gives very high accuracy and speed of making measurements.

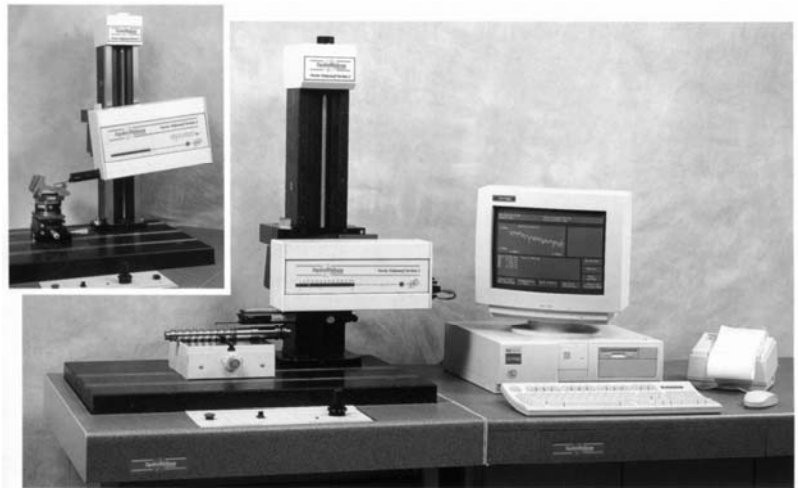

Fig. 3. Stand for stereometric investigations of surface (Taylor Hobson's profilographometer)

Its software facilitates visualization of the surface microgeometry using topographic maps (Fig. 4) or isometric images (Fig. 5). In the investigation, a sampling step of 1 μm was applied in *X* and *Y* directions with the indication accuracy of 2% or 4 nm. The scope of the measuring head in axis *Z* was 1 mm with 16 nm resolution.

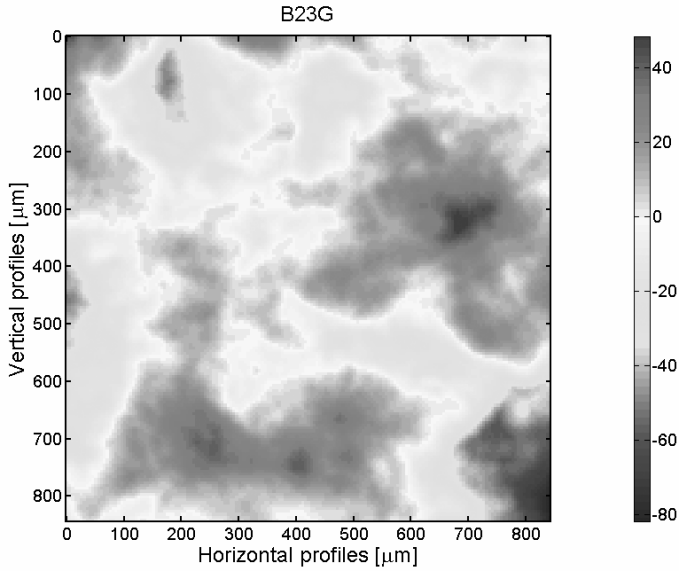


Fig. 4. Example of a topographic map of the investigated surface

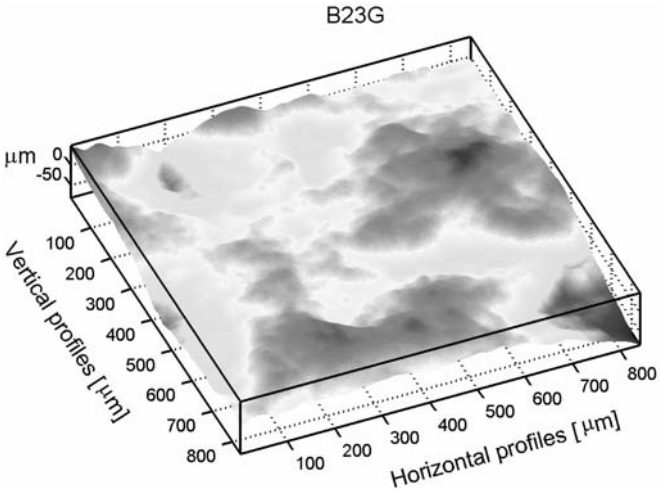


Fig. 5. Isometric view of a surface measured using a profilograph

An area of 841 μm×841 μm was investigated, from which 707 281 measuring points were obtained (Figs. 4, 5). From the whole set, singular, mutually perpendicular profile lines were selected (Fig. 6).

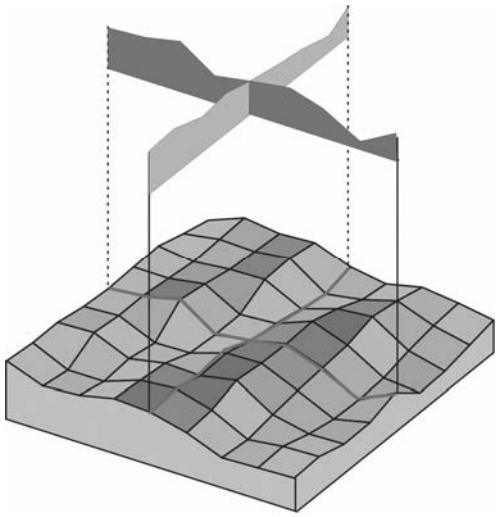

Fig. 6. Examples of mutually perpendicular fracture surface profiles

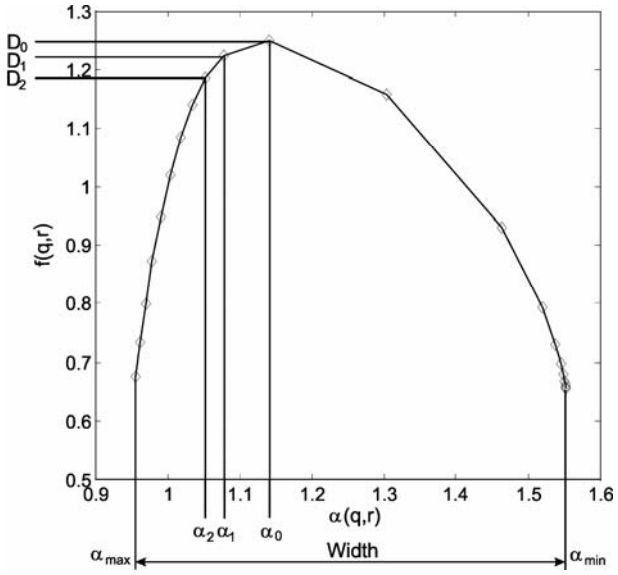


Fig. 7. Characteristic values of a multifractal spectrum. $D_0$, $D_1$, $D_2$ – some fractal dimensions: capacitive, informative and correlative, respectively; $\alpha_0$, $\alpha_1$, $\alpha_2$ – Hölder's exponents corresponding to fractal dimensions

These profiles were real equivalents of the simulated profiles obtained as a result of applying a procedure to remove overlaps. Each of the profiles was subjected to a multifractal analysis [3, 6, 8–10]. The complete procedure was applied for the profiles in two mutually perpendicular directions. Altogether, 841 profiles were examined for each direction. Values of the multifractal spectrum (Fig. 7) characteristic of

perpendicular directions were averaged (Table 2). The symbols *V* and *H*, for vertical and horizontal directions respectively, have been used in the table to distinguish between the directions. Table 3 contains averaged values for the entire surface analyzed.

Table 2. Average values of characteristic results of a multifractal analysis for each of the *V* and *H* directions[1]

| Material | $D_0$ | $\alpha_0$ | $D_1$ | $\alpha_1$ | $D_2$ | $\alpha_2$ | $\alpha_{min}$ | $\alpha_{max}$ | Width |
|---|---|---|---|---|---|---|---|---|---|
| B2 *V* | 1.0000 | 1.0004 | 0.9996 | 0.9996 | 0.9981 | 0.9986 | 1.0406 | 0.7944 | 0.2462 |
| B2 *H* | 1.0000 | 1.0004 | 0.9996 | 0.9996 | 0.9983 | 0.9988 | 1.0357 | 0.8381 | 0.1976 |
| B23G *V* | 1.0000 | 1.0003 | 0.9997 | 0.9997 | 0.9985 | 0.9989 | 1.0478 | 0.7034 | 0.3445 |
| B23G *H* | 1.0000 | 1.0002 | 0.9997 | 0.9997 | 0.9989 | 0.9992 | 1.0384 | 0.7902 | 0.2482 |
| G10 *V* | 1.0000 | 1.0007 | 0.9992 | 0.9992 | 0.9964 | 0.9974 | 1.0342 | 0.8073 | 0.2269 |
| G10 *H* | 1.0000 | 1.0003 | 0.9997 | 0.9997 | 0.9986 | 0.9990 | 1.0292 | 0.8733 | 0.1559 |
| G30 *V* | 1.0000 | 1.0003 | 0.9997 | 0.9997 | 0.9987 | 0.9991 | 1.0399 | 0.7848 | 0.2551 |
| G30 *H* | 1.0000 | 1.0006 | 0.9994 | 0.9994 | 0.9974 | 0.9981 | 1.0381 | 0.7588 | 0.2793 |
| H10 *V* | 1.0000 | 1.0004 | 0.9996 | 0.9996 | 0.9982 | 0.9987 | 1.0373 | 0.8309 | 0.2064 |
| H10 *H* | 1.0000 | 1.0001 | 0.9999 | 0.9999 | 0.9996 | 0.9997 | 1.0261 | 0.8703 | 0.1558 |
| H30 *V* | 1.0000 | 1.0003 | 0.9997 | 0.9997 | 0.9986 | 0.9989 | 1.0212 | 0.8417 | 0.1795 |
| H30 *H* | 1.0000 | 1.0000 | 1.0000 | 1.0000 | 0.9999 | 0.9999 | 1.0217 | 0.8890 | 0.1327 |
| HF6 *V* | 1.0000 | 1.0010 | 0.9989 | 0.9989 | 0.9952 | 0.9964 | 1.0198 | 0.8606 | 0.1592 |
| HF6 *H* | 1.0000 | 1.0002 | 0.9998 | 0.9998 | 0.9990 | 0.9992 | 1.0222 | 0.8570 | 0.1652 |

[1]Description of symbols used in the table see Fig. 7.

Table 3. Average values from mutually perpendicular analysis directions containing a total of 1682 profiles of the entire surface of each material grade[1]

| Material | $D_0$ | $\alpha_0$ | $D_1$ | $\alpha_1$ | $D_2$ | $\alpha_2$ | $\alpha_{min}$ | $\alpha_{max}$ | Width |
|---|---|---|---|---|---|---|---|---|---|
| B2 | 1.0000 | 1.0004 | 0.9996 | 0.9996 | 0.9982 | 0.9987 | 1.0382 | 0.8163 | 0.2219 |
| B23G | 1.0000 | 1.0003 | 0.9997 | 0.9997 | 0.9987 | 0.9990 | 1.0431 | 0.7468 | 0.2963 |
| G10 | 1.0000 | 1.0005 | 0.9995 | 0.9995 | 0.9975 | 0.9982 | 1.0317 | 0.8403 | 0.1914 |
| G30 | 1.0000 | 1.0004 | 0.9996 | 0.9996 | 0.9981 | 0.9986 | 1.0390 | 0.7718 | 0.2672 |
| H10 | 1.0000 | 1.0002 | 0.9998 | 0.9998 | 0.9989 | 0.9992 | 1.0317 | 0.8506 | 0.1811 |
| H30 | 1.0000 | 1.0002 | 0.9998 | 0.9998 | 0.9992 | 0.9994 | 1.0215 | 0.8654 | 0.1561 |
| HF6 | 1.0000 | 1.0006 | 0.9994 | 0.9994 | 0.9971 | 0.9978 | 1.0210 | 0.8588 | 0.1622 |

[1]Description of symbols used in the table see Fig. 7.

Changes of the multifractal spectrum arms' spacing as a function of distance of the analyzed profile from the beginning of thea sample are shown in Figs. 8 and 9. Significant changes in the spectrum width in perpendicular directions are visible both for the material with the highest (Fig. 8) and the lowest percentage share of overlaps (Fig. 9). The differences may result from the fact that one of the examined directions (vertical) and the crack direction converged, whereas the other (horizontal) was perpendicular to the crack direction.

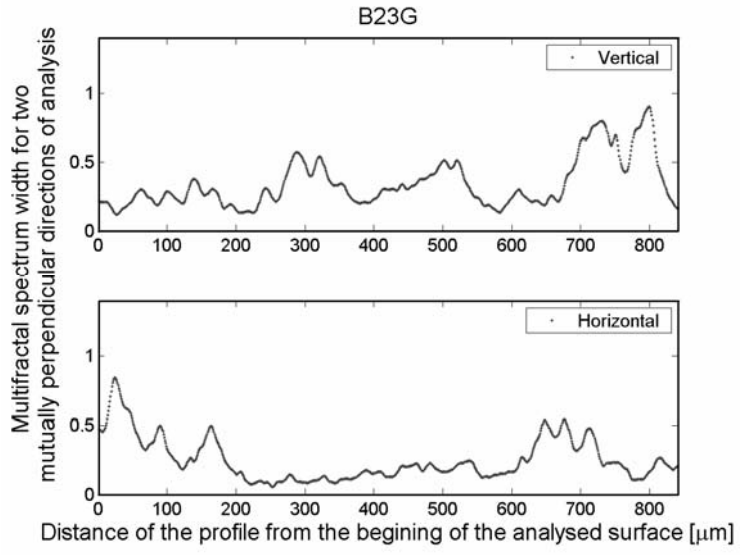


Fig. 8. Change of the multifractal spectrum width for a sample of the highest percentage share of overlaps (B23G)

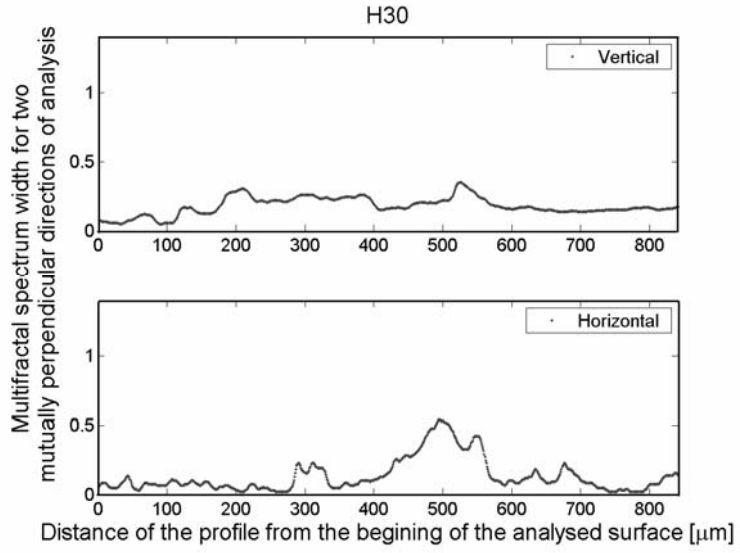


Fig. 9. Change of the multifractal spectrum width for a sample of the lowest percentage share of overlaps (H30)

The average spectrum widths obtained from the mutually perpendicular directions on the surface (the last column in Table 3) were converted (hence the name – quasi -3D) on the basis of the dependence given in [2] into adequate percentage share of overlaps (Table 4).

Table 4. Comparison of the overlap percentage share values obtained by conventional method and by applying the quasi-3D profilographometric methodology

| Material | Multifractal spectrum width (quasi-3D analysis) | Percentage share of overlaps quasi-3D (read from the correlation plot from 2D analysis) | Percentage share of overlaps (mean from four specimens, microscope) |
|---|---|---|---|
| B2 | 0.2219 | 5.60 | 7.12 |
| B23G | 0.2963 | 9.90 | 11.40 |
| G10 | 0.1914 | 3.84 | 3.31 |
| G30 | 0.2672 | 8.22 | 7.64 |
| H10 | 0.1811 | 3.24 | 4.70 |
| H30 | 0.1561 | 1.80 | 2.53 |
| HF6 | 0.1622 | 2.15 | 2.79 |

The results of the calculated percentage share of overlaps obtained by two methods are comparable, however, the quasi-3D method often shows lower values. This may result from the fact that the profilometric analysis for one profile is conducted in one direction only, whereas in the case of the quasi-3D method, the results are obtained for 841 mutually perpendicular profiles.

## 4. Conclusions

In the study, the stereometric methodology of fracture surface research was applied, supported by a multifractal analysis of mutually perpendicular profiles (quasi -3D). It has been shown that for these profiles, from material of the same grade, the width of the multifractal spectrum is different. This requires the values to be averaged in order to maintain aresults representative of the entire fracture. Measurement of such profiles by profilometry methods, using quantitative fractography to this end, enables data about the secondary cracks and overlaps to be obtained, as well as the share of individual phases in the fracture, simultaneously eliminating randomness of selection of only one, terminal profile for an analysis.

The spectrum widths averaged for both directions and converted, based on the dependence presented in [8], allow approximation, with good consistency, of the percentage share of overlaps determined by a profile analysis method. This means that the application of an algorithm to directly convert a stereometric file of a fracture surface into a multifractal one (full 3D analysis) [11] as well as verification of the solution for other material grades are purposeful. At the same time, this would allow checking the correctness of the dependence given in [8] between the spectrum width and overlaps share. It would then be possible to apply the formula so developed in further studies or directly link the crack mechanics parameters with the multifractal spectrum width as a measure of the material's fracture development.

## References

[1] ROSKOSZ S., *Zastosowanie metod stereologicznych w ocenie dekohezji węglików spiekanych*, PhD Thesis, Silesian University of Technology, Katowice, 2000.
[2] WOJNAR L., *Fraktografia ilościowa. Podstawy i komputerowe wspomaganie badań*, Politechnika Krakowska, Kraków, 1990.
[3] STACH S., CYBO J., Materials Characterization, 51 (2003), 79.
[4] MANDELBROT B.B., T*he fractal geometry of nature*, W. H. Freeman and Comp., New York, 2000.
[5] FEDER J., *Fractals*, Plenum Press, New York, 1989.
[6] CHHABRA A., JENSEN R.V., Phys. Rev. Letters, 62 (1989), 1327.
[7] HASTINGS H.M., SUGIHARA G., Fractals, *A User's guide for the natural science*s. Oxford University Press, Oxford, 1993.
[8] STACH S., ROSKOSZ S., CYBO J., CWAJNA J., Materials Characterization, 51 (2003), 87.
[9] STACH S., ROSKOSZ S., CYBO J., *Multifractal description of fracture morphology. Methodology*, unpublished.
[10] XIE H.WANG J.-A.STEIN E., Phys. Letters A, Vol. 242 (1998), 41.
[11] STACH S., CYBO J., CWAJNA J., ROSKOSZ S., Mater. Sci.-Poland, 23 (2004), 583.

*Received 6 September 2004*
*Revised 5 January 2005*